Book of Tutorials and Abstracts

European Microbeam Analysis Society

EMAS 2019

16th

EUROPEAN WORKSHOP

on

MODERN DEVELOPMENTS AND APPLICATIONS IN MICROBEAM ANALYSIS

19 to 23 May 2019
at the
NTNU, Realfagbygget
Trondheim, Norway

Organised in collaboration with:
Norwegian University of Science and Technology
(NTNU)

USING COMPLEMENTARY MICROANALYTICAL TECHNIQUES TO ANALYSE DIAMOND ANVIL CELL EXPERIMENTS

Eleanor S. Jennings

University of London, Birbeck, Department of Earth and Planetary Sciences
Malet Street, London WC1E 7HX, Great Britain
e-mail: e.jennings@bbk.ac.uk

Eleanor Jennings studied for an MSc in Geology at the University of Bristol, where she worked for a further 15 months as a research technician in the experimental laboratories, developing a diamond anvil cell (DAC) method for encapsulated melting experiments and participating in numerous DAC XRD synchrotron experiments. She completed her PhD in 2015, studying the formation of continental flood basalts through petrology and thermodynamic methods. She then spent two years working as a postdoctoral researcher at the Bayerisches Geoinstitut, an experimental petrology research institute in Bayreuth, Germany. During this time, she performed DAC and large volume press experiments examining chemical behaviour during planetary core-mantle segregation, and gained experience in FIB sample preparation and in analysing DAC experiments using EPMA, TEM, nanoSIMS and APT. Since January 2018, she has been a lecturer of geochemistry at Birkbeck, University of London, working on a range of geochemical problems on Earth and other planetary materials. She has a particular interest in EPMA, and has published nine papers on the topics of petrology/geochemistry, thermodynamic modelling, high-pressure experiments and analytical development.

1. INTRODUCTION

Diamond anvil cell (DAC) experiments are used to access the extremely high pressure and temperature conditions that are present in deep planetary interiors. These pressures are achieved by compressing samples between the truncated tips of a pair of diamonds, and very high temperatures can be reached by irradiating the sample with powerful infrared lasers [1]. DAC experiments are incredibly versatile: not only can a huge range of physical conditions be simulated, but the experimental products can also be analysed by a wide variety of techniques. In-situ measurements can be made through the diamonds, for example X-ray methods (XRF; XRD; imaging), FTIR and Raman spectroscopy. Following a high-PT experiment the sample can be extracted for additional measurements e.g., electron microbeam techniques. Multiple analytical techniques can be used in complementary way to fully interpret the experiments. For example, in-situ XRD structural measurements of high-PT phases can be interpreted with the aid of follow-up electron beam imaging and compositional measurements.

In this contribution, I begin by presenting an overview of DAC experiments. This is followed by a brief description of a selection of techniques that are used to analyse DAC experiments. I then present a series of case studies that highlight the benefits of using multiple complementary analytical techniques to interpret DAC experiments. Examples here have a focus on Earth and planetary sciences, where DAC experiments have become a popular technique to answer a wide variety of questions, ranging from phase relations and melting in the deep Earth through to mineral physical measurements that inform the quantitative analysis of geophysical measurements of planetary interiors.

2. EXPERIMENTS

To generate the pressure conditions of planetary interiors in DAC experiments, samples of a material of interest are placed between the truncated tips (culets) of two gem-quality diamonds. The diamonds are then mechanically forced together, e.g., by manually tightening screws that connect diamond backing plates, or by pressurising a membrane [1]. The force is focussed over a tiny area, generating static pressures far in excess of those generated through larger-volume techniques such as the multi-anvil press. The diamonds are mounted in such a way that light can pass into, and out of, the sample, i.e., with a cut-out in the backing plate. Pressures of up to ~ 80 GPa are routinely used; higher pressures still can be reached with very tiny truncations or through specialist tip geometries (e.g., [2]). The culets are often 100 - 300 μm in diameter, with a significantly smaller sample (e.g., 50 - 100 μm) contained within a bored-out chamber in a metal gasket (e.g., Fig. 1).

The pressure reached can be measured through the diamond using a range of in-situ microanalytical techniques. Often, a sphere or chip of ruby is included within the sample chamber. The ruby R1 emission line is fluoresced by laser, and the wavelength of this line shifts

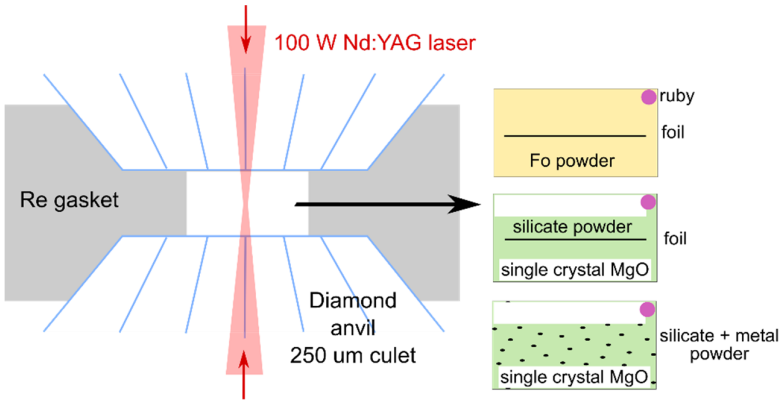

Figure 1. Example of a DAC experimental setup, designed to examine elemental distribution between molten metal and silicate (the result of such an experiment is shown in Fig. 2). Three possible sample configurations are shown on the right-hand side (not to scale). Note the ruby chip for pressure measurements and the MgO disk to insulate the diamond from the hot spot.

with pressure [3]. Alternatively, pressure can be measured by making confocal Raman spectroscopy measurements of the diamond culets themselves (e.g., [4]). Pressure determinations can also be made during experiments by making XRD measurements of materials with well-characterised equations of state such as Au, MgO or NaCl.

DAC experiments can be heated restively using electrical parts to temperatures of up to around 1,000 K, although they are more commonly heated by infrared laser in order to reach the much higher temperatures of planetary interiors. The laser-heated spot will usually be focussed on just a small area within the experimental sample of some 10s of μm diameter. Samples may need to be doped with a metal that can interact efficiently with the laser. Temperature is determined in-situ through spectro-radiometric analysis of the thermal emission spectrum over a 1D or 2D profile across the sample. Large temperature gradients result from the small laser spot and spatial variations in laser coupling efficiency, which, combined with assumptions made about emissivity, result in significant temperature uncertainties. When resistive heating is used for lower temperatures, temperature can be measured more precisely with a thermocouple (e.g., [5]). Different structural and chemical measurements can be made using a range of techniques, and complementary information can be gained by combining multiple techniques. In-situ measurements are made whilst the experiment is at high pressure, and sometimes temperature, contained between the diamonds. Such measurements include XRD, XRF and X-ray imaging because X-rays are energetic enough to penetrate the diamonds, although high-temperature measurements are significantly more technically challenging than low-temperature ones (reviewed by [6]). A synchrotron light source is usually required, and because of the difficult geometries associated with laser heating and X-ray pathways, only specialised beamlines can make measurements during laser heating [7].

Following an experiment, the sample can be carefully removed and prepared for a wider range of microbeam measurements such as electron beam methods, nanoSIMS, and atom probe measurements, in addition to X-ray techniques (e.g., Fig. 2). Such measurements can corroborate

or complement in-situ measurements: for example, combining in-situ XRD and ex-situ compositional measurements can confirm phase identities, P and T conditions, and then identify the compositions of the phases and their mixing behaviours.

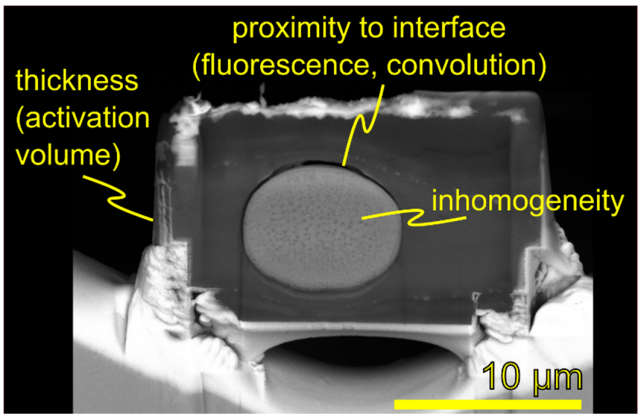

Figure 2. Example of the product of a laser-heated DAC experiment, with analytical difficulties highlighted. Here, metal and silicate were heated together and formed two immiscible liquids. Their compositions can be measured after the experiment is quenched, extracted and prepared for analysis by FIB, with an aim to define the distribution of various elements between the two phases at various PT conditions.

DAC experiments have a wide range of applications in Earth Sciences and beyond. They are used to examine phase relations within the deep silicate Earth, including its melting behaviour, composition and physical properties (e.g., [4, 8-10]). They are also used to examine metallic systems (e.g., [11-13]) and metal-silicate mixtures [12, 14-16]; Figs. 1 and 2) in order to determine the composition and properties of planetary cores and to investigate their formation conditions. Rapid quenching by switching off the laser means that equilibrium compositions of phases at high temperature are effectively "frozen in" to the experimental products.

Because of the small dimensions of the heated experimental products, there are some unique difficulties, which must be considered when analysing DAC experiments. Some techniques will be used close to their analytical limits, and care must be taken to mitigate against analytical artefacts. Effects from fluorescence, thickness and small-scale inhomogeneity must be considered (Fig. 2).

3. ANALYSING DIAMOND ANVIL CELL EXPERIMENTS: METHODS AND LIMITATIONS

In this section, a range of micro-analytical techniques that have been used, or can be used, to analyse DAC experimental products are reviewed. These focus specifically on applications suitable for the Earth and Planetary sciences.

3.1. In-situ analytical techniques

3.1.1. Synchrotron X-ray diffraction (XRD). X-ray diffraction measurements can be made using a lab X-ray source, but the far-brighter X-rays generated by a synchrotron light source are

preferable given that a proportion of the direct beam is absorbed by various DAC components other than the sample. The shorter counting times afforded by a synchrotron source allow multiple and near-continuous in-situ measurements to be made of DAC experiments, e.g., through heating and/or pressure cycles. A narrow beam will be required such that X-rays only diffract through the portion of the sample corresponding to the laser-heated spot. Typically, a diffracted monochromatic beam is detected by 2D imaging plates.

DAC experiments from which XRD measurements are made usually focus on solid materials, e.g., equation of state characterisation, synthesis experiments, and experiments to examine phase relations. Samples are usually contained within a chemically inert pressure medium (e.g., a noble gas or salt) within the sample chamber, which transmits quasi-hydrostatic pressure: Measurements of this pressure medium can be used to determine experimental pressure from material volumes. In some cases, the powdered sample itself is also the pressure medium.

Single-crystal XRD measurements can be made in the DAC: Technological developments are reviewed in detail by Boffa Ballaran et al. [5]. DACs designed with wide opening angles on the backing plates can be used to maximise the angular range of detected X-rays. Laser heating of single crystals in DAC experiments is not usually possible due to geometric constraints (but see [5] for developments), although resistive heating allows single crystal XRD conditions at elevated temperatures. Examples of applications include the characterisation of newly-synthesised phases and quantification of compression behaviour (e.g., [17-19]).

Powder XRD is frequently used to examine phase relations, equation of state and other aspects of high-PT behaviour of various materials (e.g., [20]). Some specialised beamlines allow the simultaneous laser heating and X-ray analysis of DACs, meaning that phase assemblages can be characterised in heating cycles [7]. XRD can also be applied after the heating, where experimental samples are extracted from the DAC and measured directly. Assuming that the high-pressure phases were preserved on quench and depressurisation, they can still be identified. There are many examples of application, particularly in the Earth Sciences, where phase relationships, including melting behaviour, are examined in materials representing the deep Earth's interior. The phase identities, density profiles and melting curves of pyrolytic mantle, subducted oceanic crust, and simple analogues shed light on the formation and evolution of the deep Earth and inform the interpretation of seismic data [21-25]. Phase relations in metals at planetary core conditions inform models of the composition and physical conditions of inner core crystallisation [11, 13].

Finally, developments in experimental design and data processing have allowed the quantification of the densities, local structure, and compression mechanisms of amorphous materials, especially liquids, in the DAC from direct measurements of X-ray diffuse scattering. Materials range from silicate melts [26] to molten metals [27], with application to Earth's deep interior.

XRD measurements are frequently combined with other techniques, such that phase identifications and physical properties are complemented by fully quantified compositions and spatial context (section 4).

3.1.2. Synchrotron micro-X-ray fluorescence (μ-XRF). In XRF, the fluorescence of characteristic X-rays from a material is induced by irradiation with high-energy primary X-rays. In μ-XRF, the X-ray beam is focussed to a small spot. Synchrotron radiation provides the high X-ray flux typically required for the high spatial resolution and sensitivity needed. Detection limits can be lower than for EPMA analysis. As with XRD, high-energy X-rays can penetrate through diamond, allowing XRF to be used for in-situ measurements in the DAC at high-PT conditions: This is particularly powerful for the measurement of fluids, as quenching is not required [28, 29].

Matrix corrections must be made for X-ray absorption by the sample, and secondary effects occur such as the absorption of fluoresced X-rays and subsequent emission of additional secondary X-rays (known as enhancement). The volume from which X-rays can be generated through enhancement is potentially much larger than the focussed beam spot size. This should be considered in the context of measuring small or heterogeneous materials in the DAC. Additionally, the interaction volume for each X-ray is dependent on its characteristic energy: This makes the resolution of an XRF map dependent on the energy of the X-ray, and complicated matrix corrections.

μ-XRF has been used for the in-situ measurement of many tiny geologically-relevant samples in DAC experiments where there is a requirement to physically retain a fluid phase at high-PT conditions, e.g., mineral solubility studies [28, 30]. Andrault *et al.* [31] used μ-XRF to make elemental maps with ~ 1 μm spatial resolution of a quenched DAC experiment to examine partitioning of FeO between solid phases and liquid at lower mantle conditions. μ-XRF has also been pioneered in the analysis of quenched liquid metal – liquid silicate DAC partitioning experiments, where detection limits of 2 - 5 ppm allow the analysis of strongly siderophile or lithophile elements which are trace elements in one phase [32].

3.2. Ex-situ analytical techniques

3.2.1. Focussed ion beam (FIB) sample preparation for microbeam techniques. DAC experiments can be prepared for microbeam analysis by FIB, Ar ion milling, or by conventional polishing. FIB gives fine control over the sample site and shows 3D context (for example, the lamella can be imaged front and back) [33]. For EPMA analysis, a lamella of at least several μm thickness is required – this can be subsequently thinned for TEM analysis. A dual-beam instrument allows imaging with an electron beam and milling with a Ga^+ beam. The process of cutting the site, extracting the sample, welding it to a Cu grid and thinning to the final geometry [33] is shown in Fig. 3, using a DAC experiment with a molten metal sampling region as an example. The lamella must be cleaned of implanted Ga^+ and redeposited material using a low

power Ga^+ beam. For TEM analysis, these final stages must be carefully performed to avoid beam damage [33].

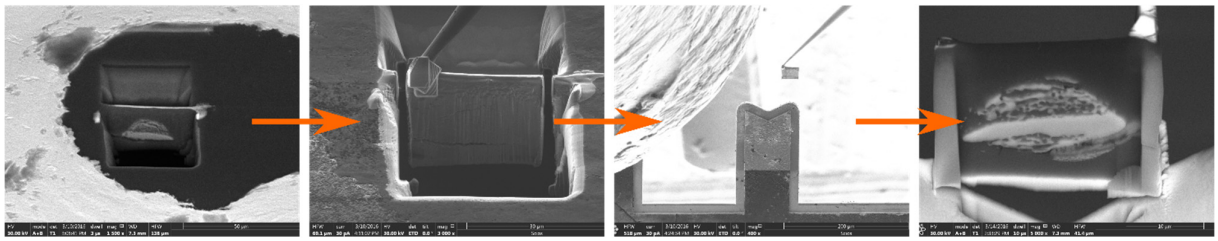

Figure 3. The process of preparing a sample as a lamella for EPMA, SEM or TEM by FIB.

A related procedure can be used to produce an ATP needle tip: 1) a wedge-shaped chunk is cut from a sample and lifted out; 2) the end of this chunk is welded to a truncated Si needle (a post) of a sample holder; 3) the beam is rastered over a ring-shaped area, that becomes successively smaller and lower current/voltage, until an extremely low power beam is used for the final sharpening to a ~ 30 nm point. A very low power beam removes traces of implanted Ga^+.

3.2.2. Electron beam methods: EPMA, FE-EPMA. EPMA is by far the most commonly used technique to perform non-destructive, small spot-size compositional analysis of solid samples, and is particularly relied upon in the Earth Sciences. It offers rapid, fully quantified analyses at micrometre-scale spatial resolutions, combined with low relative errors. A flat polished surface is required, which is traditionally achieved by mechanical polishing. Because of the small dimensions of DAC samples, a polished surface is more usually achieved through extraction of the analytical area and FIB milling.

Although EPMA is considered a routine technique, it was not originally envisaged for very small samples such as DAC samples. Users may be unaware of the limitations of EPMA for tiny samples. Difficulties stem from the fact that although the beam can be focussed to a sub-micrometre diameter on a sample surface, electrons and X-rays are able to travel and spread within the sample. The volume within which electrons can travel, interact with atoms and excite X-rays (and so generate a primary signal), the interaction volume, is ~ 1 µm diameter at typical operating conditions of 15 to 20 kV. X-rays themselves can excite secondary X-rays, and given that high energy X-rays are less impeded than electrons and can travel much further in a material, the generation of signal from 10s - 100s µm from the analytical point represents a minor, but potentially important, source of analytical error. In tiny samples, thin samples, or measurements made very close to grain boundaries, such as when analysing high pressure experimental samples, these represent the limitation of the technique [34, 35].

There are many examples of EPMA used for the measurement of DAC samples. These include partitioning studies, where two or more phases are equilibrated at temperature, quenched, and analysed [15, 36-40], with many studies focused on planetary core formation. These experiments usually involve equilibration of metals with silicates at > 30 GPa in a laser-heated DAC. The highly heterogeneous nature of these experiments, coupled with their small size, are challenging for the analyst. Sub-solidus DAC experiments usually produce crystals that are too small for easy EPMA characterisation.

An EPMA equipped with a field emission gun rather than a filament may be more appropriate for the measurement of tiny samples, as the beam can be better focussed at low accelerating voltages, reducing the interaction volume. For example, Tateno *et al.* [41] measured the composition of quenched melt in DAC melting experiments performed at lower mantle conditions using a 10 kV_{acc} beam, and Sinmyo and Hirose [42] mapped Soret diffusion in a DAC using this method, also at 10 kV_{acc}. However, whilst this offers benefits in spatial resolution, it presents difficulty with measuring higher energy characteristic X-rays such as Fe-$K\alpha_1$. Furthermore, instrumental effects such as carbon deposition must be minimised for analysis to be meaningful.

Finally, EDS measurements have also been used for measuring DAC experiments, on an SEM or EPMA instrument. For example, Chidester *et al.* [43] measured DAC experiments examining the high P-T metal-silicate partitioning of U by EDS. However, spectral resolution and detection limits are significantly better in WDS than EDS, so WDS is preferred for fully quantitative analyses. EDS is convenient and a useful tool for elemental mapping and, when fully calibrated, can be very useful for analysing major elements.

3.2.3. Transmission electron microscope (TEM). TEM involves transmitting a focussed beam of electrons through a thin sample, and the possible range of modes of use and types of analyses are dictated by the instrumentation. Spatial resolution is much higher than in an SEM (also EPMA), allowing e.g., crystallographic defects to be imaged, and crystallographic data can be obtained by electron diffraction. A very high accelerating voltage is frequently used relative to SEM/EPMA for higher resolution, since it is assumed that electron scattering is negligible during the beam's journey through the sample.

A particular adaptation of TEM, STEM (Scanning TEM), involves rastering the finely focussed beam over the sample. When combined with an analytical TEM technique (e.g., EDS, electron energy-loss spectroscopy EELS), this can be used to obtain elemental and/or chemical maps of a sample. As with SEM/EPMA, a spectrum of emitted characteristic X-rays can be measured by an EDS detector: This can be used to obtain either point analyses or maps of relative elemental concentrations of a sample at a nm-scale spatial resolution. Measurement is usually standardless and requires knowledge of *k*-factors and sample thickness to calibrate the counts. EELS relies on the fact that primary electrons that pass through the sample will lose some energy through inelastic scattering interactions with electrons from within the sample. This technique is

complementary to EDS, but is more sensitive to lower atomic number elements. Both of these techniques give better spatial resolution, but worse precision and accuracy, than WDS by EPMA, and may also be affected by fluorescence artefacts as discussed for EPMA in section 3.2.2.

In order to be analysed by TEM, samples must be electron-transparent (e.g., ~ 100s nm thick, material- and accelerating voltage-dependent). Geological samples can be prepared by FIB or by ion milling [33, 44]. Sample preparation for TEM is generally more difficult and time-consuming than for EPMA/SEM.

STEM with EDS and EELS has long been used to measure elemental concentrations in many tiny natural geological samples and DAC experiments. Frost *et al.* [45] analysed DAC experiments to examine O distribution between quenched liquid iron veins and solid magnesiowüstite. Fischer *et al.* [16] analysed quenched liquid metal – liquid silicate DAC partitioning experiments using a broader spot size of 0.5 - 2 μm (to integrate fine quench textures). In both cases, STEM was used, with relative elemental concentrations determined by standardless EDS, and relative O ± C concentrations determined by EELS.

3.2.4. Atom probe tomography (APT). APT is a powerful technique, allowing the identification and 3D mapping of individual atoms in a sample (reviewed elsewhere e.g., [46]). However, it is also amongst the most difficult, expensive and time-consuming techniques in terms of sample preparation and analytical success. It is best suited to one-off measurements, and is more successful for conductive materials, which better withstand the analytical conditions. Samples are on the order of 100s nm and features at the sub-nm (atomic) scale are resolvable, so this is best suited for when extremely high spatial resolution is required. A sample must be prepared as a sharp needle tip. The evaporated atoms are ionised and identifiable by their mass/charge ratio (i.e., isotopic identification is possible). Detection efficiency is very high, and using the position and relative timing of counts, a 3D image is reconstructed.

APT is not routinely used in the Earth Sciences because insulating materials are not best suited to the high field gradients. It has, however, occasionally been applied to natural samples where nm-scale 3D resolution and compositional identification are required. Some notable examples include: i) characterising Pb nanoclusters within Earth's oldest zircon [47]; ii) the U-Pb dating of impact and crystallisation events from discrete nanostructural domains in baddeleyite [48]; iii) developments in APT that are being made towards the characterisation of the C isotopic composition of pre-solar nanodiamonds (e.g., [49]). In section 4.2, an APT measurement of exsolution within quenched metal from a DAC experiment is presented.

3.2.5. Nanoscale secondary ion mass spectrometry (nanoSIMS). SIMS relies on a primary ion beam (e.g., O^- or Cs^+) that bombards the sample and sputters ionised material; these secondary ions are analysed by a mass spectrometer. It can be effective for both chemical mapping and spot analyses. NanoSIMS is a variant of SIMS optimised for nanoscopic scale spatial resolution, with theoretical resolutions of around ~100 nm [50]. Like SIMS, it has the advantage of making

isotopic as well as elemental measurements. However, using a very small spot size compromises on analytical sensitivity. SIMS techniques depend on appropriate standardisation, as the ionisation efficiency of various elements is matrix-dependent, so closely matrix-matched standards are needed to convert counts to composition. In nanoSIMS, even variations in surface topography and sample morphology can cause offset relative to standards: Analyses have a reputation for being difficult. SIMS/nanoSIMS require a highly polished surface for analysis.

NanoSIMS is a well-known technique for tiny samples, and is particularly used for its isotopic analysis capability: Instrumentation and examples of used are reviewed in detail elsewhere [50]. Examples include cosmochemical studies of extra-terrestrial materials such as presolar grains [51]. NanoSIMS has also been used in the chemical analysis of DAC experiments when a high spatial resolution or light element measurement is required [52]; recently, Suer *et al.* [53] quantified the S content of run products in DAC metal-silicate partitioning experiments. However, the trade-off between sensitivity and analytical resolution is ever-present whilst matrix matching of exotic materials, and in particular metals derived from very high pressure experiments, is not trivial.

4. COMBINED APPROACHES

4.1. Introduction

Each technique described in section 3 can be used in isolation to analyse DAC experiments. However, when used in combination, complementary techniques are hugely powerful in extracting more information from experiments and verifying observations of these tiny samples. For example, whereas XRD provides material structural data (phase identification, structure, unit cell parameters), it cannot provide compositional data. Other techniques such as electron microbeam methods and XRF provide compositional data, but not structural. Finally, different resolutions can be accessed through different techniques, such that "bulk" measurements that are assumed to be homogeneous on the μm-scale can be further interrogated for spatial variations at the nm-scale using TEM, APT and nanoSIMS. In the following section, some case studies are highlighted where complementary techniques were required to fully interpret DAC experiments.

4.2. Case studies

4.2.1. Chemistry and mineralogy of Earth's lowermost mantle. A seismic discontinuity, known as D″, exists near the base of the Earth's mantle, a few hundred kilometres above the core-mantle boundary. It is seismically anisotropic and is characterised by an step increase in seismic velocity, although the lowermost mantle more generally is known to be seismologically complex [54]. Following the discovery of a new deep-mantle phase transition by Murakami *et al.* [23], this discontinuity is now explained by the transformation of bridgmanite to a post-perovskite

structure. Post-perovskite was observed and characterised by Murakami *et al.* [23] using in-situ synchrotron XRD measurements of laser-heated DAC experiments up to 134 GPa and 2,600 K. Soon after, Murakami *et al.* [55] used similar high-PT DAC experiments on a pyrolite composition to both better characterise phase relations, and to make compositional measurements of the phases. Using in-situ XRD followed by Ar ion thinning and TEM EDS analysis, they determined that Fe is significantly less compatible in post-perovskite than in perovskite, shifting the distribution of Fe and Mg between phases at the transition. Additionally, the authors observe that the Mg/Fe ratio in bridgmanite relative to periclase is higher when measured by electron beam methods than when inferred directly from unit cell changes measured by XRD [56], highlighting the benefit in combining multiple analytical methods to verify results.

4.2.2. Melting and crystallisation in a deep magma ocean. Melting and crystallisation are a fundamental mechanism by which planets differentiate into their component layers, where deep magma ocean crystallisation and/or melting can drive chemical fractionation. Additionally, there may be seismological evidence for low the presence of low-degree melts in present day Earth's lower mantle [54]. In order to understand the compositional consequences of deep melts and their physical plausibility, high pressure experiments are needed to examine phase relations, melt compositions and melt properties.

Tateno *et al.* [41] used high-PT DAC experiments to generate melts in equilibrium with pyrolytic mantle up to 179 GPa. They analysed phases in quenched samples by FE-EPMA and additionally verified phase identifications in some samples by XRD. It was found that partial melts became increasingly Fe-rich with pressure, which was mirrored by a drop in Fe/Mg in bridgmanite and an even lower Fe content in post-perovskite. The resultant high Fe content predicted for low-degree melts means that they would be dense and negatively buoyant deeper than 2,000 km, i.e., they would be trapped at the base of the mantle. This conclusion contrasts that of Andrault *et al.* [31], who ran similar experiments but analysed recovered samples by creating simultaneous XRF and XRD maps, allowing them to identify the phases present in each pixel and assign XRF compositions accordingly. Andrault *et al.* [31] found liquid compositions that were lower in FeO than those of Tateno *et al.* [41]. For a more accurate perspective on mantle melting temperatures, Nomura *et al.* [57] used ex-situ X-ray micro-tomographic imaging to identify the onset of melting, where the Fe-rich nature of the melt (as confirmed by FE-EPMA) meant that an X-ray energy bracket could be selected to image Fe-rich regions as a proxy for melt. Despite differences in techniques and conclusions, it is clear that combining multiple analytical methods is a powerful approach in measuring melting experiments.

4.2.3. Linking subducted oceanic crust to ultradeep diamond genesis. Until recently, there have been no samples of subducted material from the lower mantle. However, a set of rare "ultradeep" diamonds from Brazil were found to contain unusual mineral assemblages (e.g., nepheline, kalsilite, ulvöspinel, $CaSiO_3$, pyroxenes and olivine) trapped as tiny inclusions within the crystals [25, 58]. Many inclusions contain multiple phases. Compositions were characterised using EPMA and Raman spectroscopy, and it was concluded that the polyphase inclusions

represent single lower mantle phases that unmixed during decompression [25]. However, the re-integrated composite inclusions often still had unusual compositions relative to known mantle phases: for example, the Na- and K- rich compositions correspond to phases known as "CF" and "NAL", which are not present in ambient mantle peridotite, and led Walter *et al.* [25] to conclude that the composite inclusions represent crystals from deeply-subducted oceanic crust that were trapped during diamond growth. They represent the first direct evidence of whole-mantle recycling of ancient material.

Walter *et al.* [25] supported their conclusions using phase relations determined by previous high-PT DAC experiments performed on basaltic compositions [24] alongside lower-P experiments. The study also resulted in further experiments being performed, to better understand the inclusions' origins (e.g., [59, 60]). In one such study, we performed laser-heated DAC experiments to examine the effect of K on stability of the unusual diamond-hosted NAL and CF phases. XRD measurements identified both phases, but in some experiments, additional K-hollandite and an unknown phase were identified: this number of phases should not have been stable from thermodynamic arguments. Follow-up STEM EDS (Fig. 4) and TEM electron diffraction measurements allowed the identification and quantification of the compositions of all phases, helping to better constrain phase boundaries. The unknown phase was probably δ-AlOOH, where the unexpected presence of water had allowed the stabilisation of an additional phase. Occasional 120° triple junctions confirmed that the experiments reached equilibrium. Combining XRD measurements with follow-up microbeam work were a powerful way to interpret and confirm unexpected results.

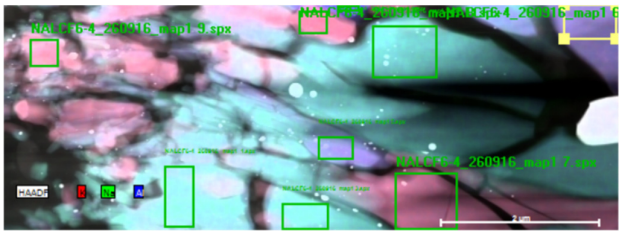

Figure 4. STEM EDS map a sample that was equilibrated at sub-solidus conditions, containing NAL and K-hollandite (pink/Al+K-rich), CF (green/Na-rich), and an aluminous phase (blue). Scale bar 2 µm.

4.2.4. Metal-silicate partitioning experiments to investigate the composition of planetary cores: characterisation of nm-scale textures. The conditions involved in the accretion of Earth and segregation of its core can be investigated by interpreting the depletions of various siderophile (iron-loving) elements in its silicate layers (e.g., [61]). For this, we must know how the various elements distribute themselves between molten metal and silicate, and how that distribution changes as a function of pressure, temperature and composition. The quest to extend partitioning experiments to lower-mantle conditions has necessitated the use of laser-heated DAC experiments. Usually, such experiments are run by sandwiching a small flake of iron metal foil between disks of silicate glass or compressed powder, where one or both phases are doped with elements of scientific interest [16, 38, 53].

Because the focus of such experiments is compositional, the samples are analysed following rapid quench, extraction and FIB preparation. The experimental run products invariably consist of a central metal sphere (~ 5 - 10 µm diameter) with a quenched silicate melt rim (~ 1 - 5 µm wide; Fig. 5). Phases frequently contain entrained or exsolved blebs (Fig. 2): Whether these should be avoided during analysis depends on the interpretation of their origin. The compositions of experimental run products are typically measured by WDS by EPMA [14, 15, 36-38, 40] or EDS [43], although other studies utilised TEM or nanoSIMS [16, 45, 53]. The small sample size and geometry presents unique analytical challenges that are especially problematic in experiments where element partitioning between coexisting chemically and physically dissimilar phases is desired [34, 35].

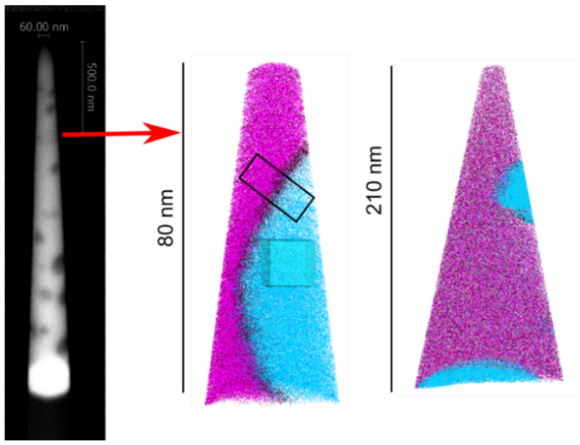

Figure 5. Left: BSE image of a needle cut by FIB for APT measurement of a DAC experimental metal containing an immiscible silicate phase. The oxide spheres and Fe-rich matrix are clearly visible. Needle is around 2 µm long from the white Pt base, and 60 nm wide just below the tip. Right: APT reconstruction of the positions and identities of the atoms in two needles from the same experiment. Fe - pink; C - maroon; O - light blue; Si- grey. Trace elements not shown. Black rectangle is position of the proxigram cylinder (see Fig. 6).

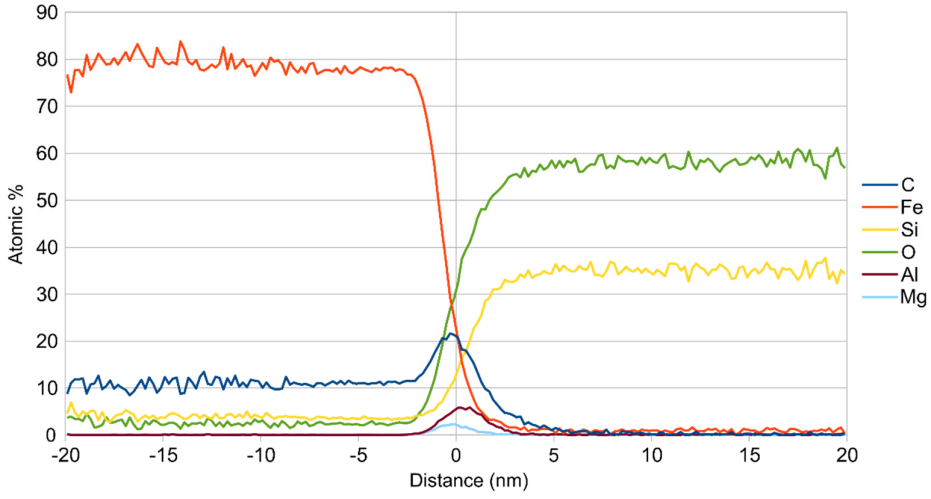

Figure 6. Proxigram (average at% concentrations) through the cylinder marked in Fig. 5, binned as a function of distance to a curved iso-surface of Si concentration. Three regions are seen: Left, C-bearing Fe metal matrix; centre, interface rich in trace elements and C; Right, almost stoichiometric SiO_2 in the interior of the sphere. Matrix and sphere are very homogeneous.

An interesting aspect to using multiple analytical techniques is the ability to measure at different spatial scales. The metal phase in metal-silicate partitioning experiments characteristically contains small (10s - 100s nm) spheres of a silicate material that are more clearly visible by TEM than BSE imaging. A typical approach is to interpret these spheres as quench exsolution and use a "broad" (e.g., 1 μm) electron beam to integrate these with the host metal for a bulk phase composition. This approach indicates a high simultaneous solubility of Si and O within Fe metal at core formation conditions (e.g., [37]). However, this conclusion relies on an assumption that the Si-O-rich spheres exsolved during quench and were soluble at high temperature. In order to characterise the spheres and any compositional gradients around their interfaces, a DAC experiment quenched metal was analysed by APT, giving several orders of magnitude higher spatial resolution in 3D space. It was determined that the spheres were pure stoichiometric SiO_2, that only low levels of Si and O remained in the metal, and that there were no compositional gradients in Si or O leading to the interface with the spheres [62]. This may cast doubt on the origin of the spheres: If they were dynamically stable throughout the experiment, then experimental interpretation in terms of the solubility of Si and O in planetary cores must be revisited.

4.2.5. Extreme thermal and chemical gradients in DAC experiments. One major advantage in combining ex-situ micro-analytical techniques with e.g., in-situ XRD has been in highlighting the limitations of the DAC technique, and informing the interpretation of XRD data.

It is well-known that thermal gradients in laser-heated DAC experiments are large: This is a consequence of laser heating, where radiation interacts with a laser-absorbing material. If the beam has a Gaussian profile, the centre will naturally be hottest, although beam-shaping optics are commonly used to counter this [63]. Homogeneous heating is especially difficult when working with a sample that is physically mixed with a metal to interact with the laser, or when a material begins to melt, allowing the re-distribution of material and resulting in heterogeneous heating.

The thermal profile can be used as an advantage. For example, Tateno *et al.* [41] qualitatively use distance from the heating spot as a proxy for temperature, and interpret their concentric pattern of phase stability as mirroring crystallisation sequence, thus maximising the information retrieved from their experiments. However, this highlights the importance of aligning the X-ray beam and the laser-heated spot precisely for in-situ measurements of heated DAC experiments, else the measured XRD pattern may be recording additional peaks from lower-temperature phases peripheral to the area of interest.

Ex-situ micro-analytical work using a small spot size has highlighted a particular chemical consequence of heterogeneous heating. Diffusion can be driven by a temperature gradient: this thermal diffusion is known as Soret diffusion. In silicates in DAC experiments, it appears that Fe, Al and K migrate in the direction from hot to cold; Si appears enriched in the hot spot; and Mg can migrate in either direction, dependent on material (Fig. 7; [42]). This affects solid

samples as well as liquids. Samples are most affected when a laser-absorbing powder is mixed into the sample, and can be mitigated against with metal coatings or no laser absorber, insulation layers, and short experimental run times [42]. Soret diffusion may not be identified in XRD measurements and poses a major difficulty in interpreting DAC experiments, especially when melting is involved. A homogeneous starting material may no longer be homogeneous, changing the stabilities of various phases: for example, a localised concentration of MgO will increase the stability of ferropericlase [41], and a higher concentration of FeO may decrease the melting temperature. Soret diffusion provides an additional hypothesis for the presence of concentric structures around laser-heated spots, and may be responsible for some of the discrepancies between different studies [42].

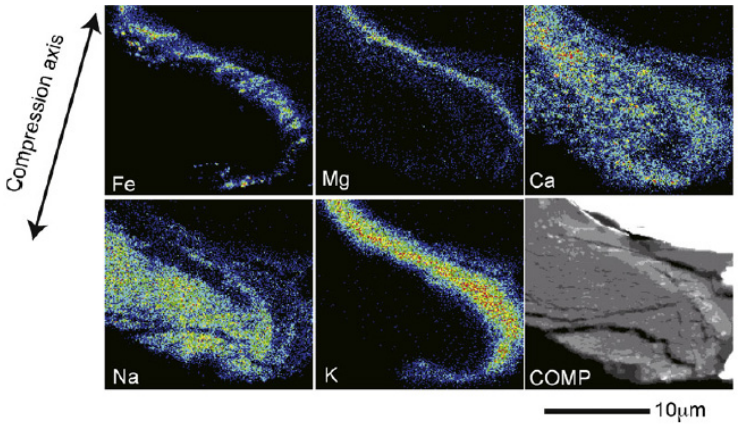

Figure 1. Extreme chemical segregation within an initially homogeneous granitic composition due to thermal diffusion. Fe, Mg and K have migrated away from the hottest region [42]. Sample was heated at 1,900 K for 63 minutes.

Problems with diffusion and changes to the localised bulk composition can be checked by following up in-situ XRD measurements with ex-situ imaging and compositional measurements. Variations in the localised "bulk" compositions may indicate a problem.

5. CONCLUSION

DAC experiments allow various materials to be held at the static pressures found deep in planetary interiors, and their popularity is in part due to their ease of use. Samples can be heated to extreme temperatures and allow are amenable to a huge range of analytical techniques. DAC experiments have found particular popularity in the Earth and planetary sciences, as well as in materials sciences, chemistry, and biological materials. Measurements can be made through the diamond anvils, either optically or using a synchrotron X-ray source, and additional measurements can be made after the experiment by extracting the sample. The main limitations of DAC experiments are the very small sample size and the high potential for heterogeneous heating and diffusion. Using just XRD for a laser-heated experiment could miss important features such as disequilibrium and diffusion. By combining in-situ and ex-situ techniques,

experimental products can be fully characterised. An ideal case could consist of in-situ XRD to identify the high-PT phases, confirm PT conditions and to refine equation of state; followed by ex-situ micro- and nanoscale imaging and compositional measurements, to relate XRD measurements to experimental textures and to characterise phase compositions and elemental distribution within the DAC experiment.

6. REFERENCES

[1] Jayaraman A 1983 *Rev. Mod. Phys.* **55** 65-108
[2] Dubrovinsky L, Dubrovinskaia N, Prakapenka V B and Abakumov A M 2012 *Nature Commun.* **3** 1163
[3] Mao H K, Xu J and Bell P M 1986 *J. Geophys. Res. Solid Earth* **91** 4673-4676
[4] Walter M J, *et al.* 2015 *Chem. Geol.* **418** 16-29
[5] Boffa Ballaran T, Kurnosov A and Trots D 2013 *High Press. Res.* **33** 453-465
[6] Shen G and Mao H K 2017 *Rep. Prog. Phys.* **80** 016101
[7] Ohishi Y, *et al.* 2008 *High Press. Res.* **28** 163-173
[8] Baron M A, *et al.* 2017 *Earth Planet. Sci. Lett.* **472** 186-196
[9] Hirose K, Fei Y, Ma Y and Mao H-K 1999 *Nature* **397** 53-56
[10] Kesson S E, Fitz Gerald J D and Shelley J M 1998 *Nature* **393** 252-255
[11] Lord O T, *et al.* 2010 *J. Geophys. Res. Solid Earth* **115** B06208
[12] Lord O T, *et al.* 2009 *Earth Planet. Sci. Lett.* **284** 157-167
[13] Morard G, *et al.* 2017 *Earth Planet. Sci. Lett.* **473** 94-103
[14] Badro J, Siebert J and Nimmo F 2016 *Nature* **536** 326-328
[15] Bouhifd M A and Jephcoat A P 2003 *Earth Planet. Sci. Lett.* **209** 245-255
[16] Fischer R A, *et al.* 2015 *Geochim. Cosmochim. Acta* **167** 177-194
[17] Boffa Ballaran T, *et al.* 2012 *Earth Planet. Sci. Lett.* **333-334** 181-190
[18] Lavina B, *et al.* 2011 *Proc. Natl. Acad. Sci.* **108** 17281-17285
[19] Mao Z, *et al.* 2012 *Earth Planet. Sci. Lett.* **331-332** 112-119
[20] Knittle E and Jeanloz R 1987 *Science* **235** 668-670
[21] Fiquet G, *et al.* 2000 *Geophys. Res. Lett.* **27** 21-24
[22] Hirose K, Takafuji N, Sata N and Ohishi Y 2005 *Earth Planet. Sci. Lett.* **237** 239-251
[23] Murakami M, *et al.* 2004 *Science* **304** 855-858
[24] Ricolleau A, *et al.* 2010 *J. Geophys. Res. Solid Earth* **115** B08202
[25] Walter M J, *et al.* 2011 *Science* **334** 54-57
[26] Sanloup C, *et al.* 2013 *Nature* **503** 104-107
[27] Morard G, *et al.* 2013 *Earth Planet. Sci. Lett.* **373** 169-178
[28] Schmidt C and Rickers K 2003 *Amer. Mineralogist* **88** 288-292
[29] Petitgirard S, *et al.* 2009 *Rev. Sci. Instrum.* **80** 033906
[30] Manning C E, Wilke M, Schmidt C and Cauzid J 2008 *Earth Planet. Sci. Lett.* **272** 730-737
[31] Andrault D, *et al.* 2012 *Nature* **487** 354-357

[32] Petitgirard S, *et al.* 2012 *Rev. Sci. Instrum.* **83** 013904
[33] Wirth R 2009 *Chem. Geol.* **261** 217-229
[34] Jennings E S, Wade J, Laurenz V and Petitgirard S 2019 *Microsc. Microanal.* **25** 1-10
[35] Wade J and Wood B J 2012 *Phys. Earth Planet. Inter.* **192-193** 54-58
[36] Bouhifd M A and Jephcoat A P 2011 *Earth Planet. Sci. Lett.* **307** 341-348
[37] Siebert J, Badro J, Antonangeli D and Ryerson F J 2012 *Earth Planet. Sci. Lett.* **321-322** 189-197
[38] Blanchard I, Siebert J, Borensztajn S and Badro J 2017 *Geochem. Perspect. Lett.* **5** 1-5
[39] Siebert J, *et al.* 2018 *Earth Planet. Sci. Lett.* **485** 130-139
[40] Mahan B, *et al.* 2018 *Geochim. Cosmochim. Acta* **235** 21-40
[41] Tateno S, Hirose K and Ohishi Y 2014 *J. Geophys. Res. Solid Earth* **119** 4684-4694
[42] Sinmyo R and Hirose K 2010 *Phys. Earth Planet. Inter.* **180** 172-178
[43] Chidester B A, Rahman Z, Righter K and Campbell A J 2017 *Geochim. Cosmochim. Acta* **199** 1-12
[44] Miyajima N, *et al.* 2010 *J. Microscopy* **238** 200-209
[45] Frost D J, *et al.* 2010 *J. Geophys. Res. Solid Earth* **115** B02202
[46] Gault B, Moody M P, Cairney J M and Ringer S P 2012 *Atom probe microscopy*. (New York, NY: Springer Science & Business Media)
[47] Valley J W, *et al.* 2014 *Nature Geosci.* **7** 219-223
[48] White L F, *et al.* 2017 *Nature Commun.* **8** 15597
[49] Lewis J B, Isheim D, Floss C and Seidman D N 2015 *Ultramicroscopy* **159** 248-254
[50] Kilburn M R and Wacey D 2014 in: *Principles and practice of analytical techniques in Geosciences*. (London, UK: Royal Society of Chemistry). 1-34
[51] Zinner E 2007 in: *Treatise on geochemistry*. (Holland H D and Turekian K K; Eds.). (Oxford, UK: Pergamon Press). 1-33
[52] Badro J, *et al.* 2007 *Earth Planet. Sci. Lett.* **262** 543-551
[53] Suer T-A, *et al.* 2017 *Earth Planet. Sci. Lett.* **469** 84-97
[54] Garnero E J and McNamara A K 2008 *Science* **320** 626-628
[55] Murakami M, Hirose K, Sata N and Ohishi Y 2005 *Geophys. Res. Lett.* **32**
[56] Andrault D 2001 *J. Geophys. Res. Solid Earth* **106** 2079-2087
[57] Nomura R, *et al.* 2014 *Science* **343** 522-525
[58] Harte B 2010 *Mineral. Mag.* **74** 189-215
[59] Armstrong L S and Walter M J 2012 *Eur. J. Mineralogy* **24** 587-597
[60] Cerantola V, *et al.* 2017 *Nature Commun.* **8** 15960
[61] Walter M J, Newsom H E, Ertel W and Holzheid A 2000 in: *Origin of the Earth and Moon*. (Tucson, AZ: University of Arizona Press). 265-289
[62] Jennings E S, *et al.* 2018 in: *EGU General Assembly 2018*. 19120
[63] Prakapenka V B, *et al.* 2008 *High Press. Res.* **28** 225-235